CAUCHY – Jurnal Matematika Murni dan Aplikasi
Volume 11 (1) (2026), Pages 1139-1154
p-ISSN: 2086-0382; e-ISSN: 2477-3344

Qualitative and Numerical Analysis of an SVEIR Model for HIV-HBV Co-Infection

Maria Lobo*, Adelya Hanaya Mage, and Ariyanto

Faculty of Science and Engineering, Department of Mathematics, Universitas Nusa Cendana, Kupang 85228, Indonesia

Abstract

The dynamics of HIV-HBV co-infection present significant epidemiological challenges, particularly in resource-limited areas. This study employs the SVEIR mathematical model to explore the transmission and control of HIV-HBV co-infection in Kupang City, Indonesia. Using the Next Generation Matrix method, the basic reproduction number (R_0) was estimated at 1.36, indicating persistent disease transmission without effective intervention. Sensitivity analyses identified HBV vaccination coverage and treatment accessibility as critical parameters significantly influencing infection dynamics. Numerical simulations validated the theoretical model, demonstrating that increased vaccination rates and enhanced antiviral therapy access substantially reduce co-infection prevalence. Furthermore, equilibrium analyses revealed that effective interventions capable of lowering R_0 below unity could transition the system from persistent endemicity toward disease elimination. These results emphasize the necessity of integrated intervention strategies, including expanded HBV vaccination, improved antiviral therapy access, and comprehensive community education to mitigate HIV-HBV co-infection. Future research should address existing limitations, incorporating behavioral and socioeconomic determinants to enhance model accuracy and applicability.

Keywords: SVEIR Modeling; HIV; Hepatitis B; Co-infection; Basic reproduction number; Vaccination; Antiretroviral therapy.

1. Introduction

Infectious diseases remain a significant global health challenge, with HIV (Human Immunodeficiency Virus) and Hepatitis B virus (HBV) among the most concerning due to their widespread prevalence and severe clinical implications. Recent global health reports emphasize that HIV and HBV continue to cause substantial morbidity and mortality, especially in resource-limited regions. Globally, approximately 38 million people were living with HIV in 2022, with Indonesia reporting one of the highest HIV burdens in Southeast Asia [1]. Additionally, WHO data indicate that an estimated 296 million individuals worldwide live with chronic HBV infection, highlighting the urgency for effective disease control and prevention strategies [2].

Co-infection with HIV and HBV presents unique epidemiological and clinical challenges, accelerating liver disease progression and complicating patient management. Individuals co-infected with both viruses have a significantly increased risk of developing severe liver conditions,

*Corresponding author. E-mail: maria_lobo@staf.undana.ac.id

Submitted: January 06, 2026 Reviewed: February 18, 2026 Accepted: May 06, 2026
DOI: https://doi.org/10.18860/cauchy.v11i1.40185

including cirrhosis and hepatocellular carcinoma, compared to individuals infected solely with HBV [3, 4]. The complexity of managing HIV-HBV co-infection arises partly from interactions between the two viruses, particularly the immunosuppressive effects of HIV, which facilitate more aggressive HBV replication and liver damage. Moreover, certain antiretroviral therapies (ART) effective against HIV also influence HBV viral load, underscoring the need for integrated treatment strategies [3, 4].

Mathematical modeling has become a pivotal tool in infectious disease epidemiology, enabling researchers and policymakers to gain deeper insights into disease transmission dynamics and evaluate intervention strategies efficiently. Traditional single-disease models fail to capture complexities inherent in co-infection scenarios. Recent studies have thus highlighted the importance of employing advanced modeling frameworks to address these gaps [5, 6]. In this context, the SVEIR (Susceptible, Vaccinated, Exposed, Infected, Recovered) model offers an ideal structure to study HIV-HBV co-infection dynamics, particularly due to its inclusion of vaccination and multi-stage disease progression compartments.

Vaccination remains a cornerstone in controlling HBV infection and subsequently reducing coinfection risks. Extensive research has consistently demonstrated that increased HBV vaccination coverage significantly reduces the transmission and prevalence of co-infection [7]. Furthermore, ART has shown significant efficacy not only in controlling HIV progression but also in indirectly mitigating HBV-related liver damage, thereby reducing overall morbidity and mortality rates in co-infected populations [8].

However, while the importance of modeling and interventions is well-established, sensitivity analyses have often been overlooked despite their critical role in enhancing model robustness and intervention optimization. Sensitivity analyses allow researchers to identify the most influential factors affecting disease spread and intervention effectiveness, thereby guiding targeted and cost-effective public health strategies [9, 10]. Previous mathematical modeling studies, such as those by [11] and [12], primarily focused on HIV-HCV co-infections without comprehensive sensitivity analyses, leaving critical knowledge gaps. We focus on HIV-HBV rather than HIV-HCV co-infection because HBV has a widely available and highly effective vaccine, making vaccination a central and actionable control lever that can be explicitly modeled and evaluated. In contrast, there is no prophylactic vaccine for HCV, so HIV-HCV models typically emphasize treatment-only strategies and different policy questions.

Moreover, the co-infection models in [11, 12] focus on HIV–HCV dynamics, where vaccination is not part of the control structure and thus cannot be used to assess HBV-specific immunization policies. In contrast, this study addresses HIV–HBV co-infection by explicitly incorporating an HBV-vaccinated class and linking vaccination coverage to the reduction of HBV infection and HBV superinfection risk among individuals living with HIV. This explicit vaccination–co-infection linkage enables a clearer prioritization of control levers through sensitivity indices and intervention simulations.

Addressing these limitations, we develop and analyze an SVEIR-type model for HIV–HBV co-infection tailored to Kupang City, Indonesia. The novelty of the formulation lies in: (i) a clinically motivated directional superinfection assumption in which HIV-infected individuals can acquire HBV (while HBV infection does not necessarily imply HIV acquisition); (ii) an explicit HBV vaccination compartment that provides complete protection against HBV while vaccinated individuals remain susceptible to HIV infection; and (iii) the assumption that HBV recovery is confined to HBV mono-infection, whereas co-infected individuals do not independently clear HBV due to weakened immunity. Analytically, we derive the basic reproduction number using the Next Generation Matrix method and decompose it into HIV and HBV transmission contributions, followed by normalized forward sensitivity indices to rank the most influential parameters. Finally, numerical simulations are used to validate the model against empirical epidemiological data from Kupang City and to evaluate intervention scenarios (e.g., increased vaccination coverage and improved HBV treatment access) that yield locally interpretable public

health recommendations.

2. Methods

To comprehensively analyze the dynamics of HIV-HBV co-infection and assess potential control measures, this study employed the SVEIR (Susceptible, Vaccinated, Exposed, Infected, Recovered) compartmental mathematical model. This model was selected for its capability to represent various health states within the population, effectively incorporating vaccination and the progression stages of disease transmission.

The SVEIR model is particularly valuable for epidemiological modeling because it captures interactions among susceptible, vaccinated, exposed, infected, and recovered populations in disease dynamics studies [13, 14]. The diagram of the model showing the HIV-HBV transmission dynamics is presented in Fig. 1.

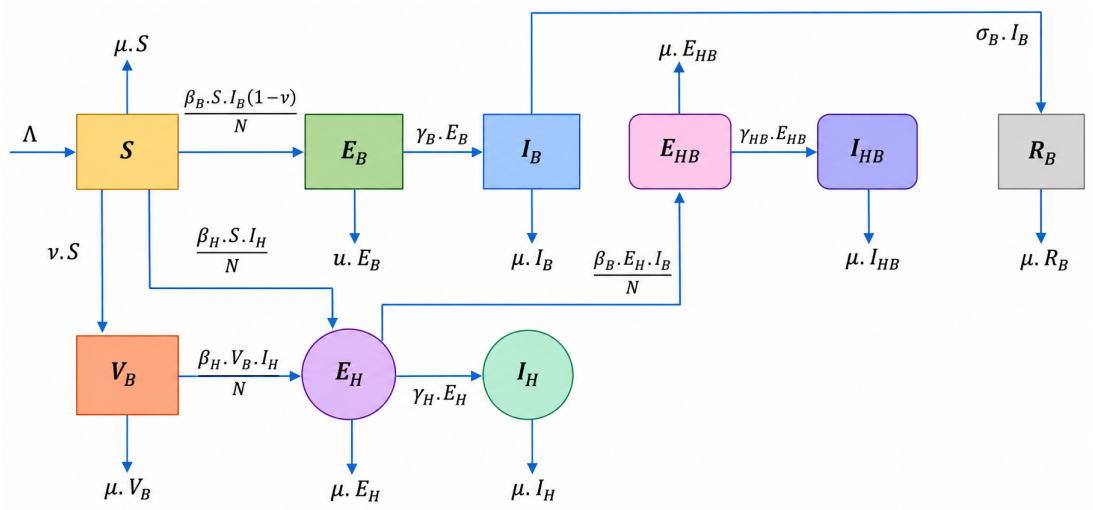

Fig. 1: HIV and Hepatitis B Co-Infection Disease Distribution Diagram

Several realistic assumptions were made in the model formulation to reflect accurately the epidemiological dynamics of HIV and HBV transmission. Individuals enter the population through recruitment at rate Λ and experience natural mortality at rate μ in all compartments. All individuals enter as susceptible and may transition through various states over time depending on exposure and interventions. Transmission mechanisms modeled include those via blood, bodily fluids, and sexual contact, consistent with established epidemiological understanding [1, 15].

An essential component of the model is the directional co-infection scope adopted in this study: HIV-exposed/infected individuals may acquire HBV (superinfection), while acquisition of HIV from HBV-only compartments is not included in the transition structure. This modeling choice reflects clinical evidence that HIV-induced immunosuppression increases vulnerability to subsequent infections such as HBV [3, 4]. Vaccinated individuals are assumed to have complete protection against HBV but remain susceptible to HIV infection, consistent with evidence on HBV vaccine effectiveness [16]. Individuals who recover from HBV acquire permanent immunity to HBV but remain susceptible to HIV, whereas co-infected individuals are assumed not to independently clear HBV due to weakened immunity.

2.1. State variables and parameters

Let $S(t)$, $V_B(t)$, $E_H(t)$, $E_B(t)$, $E_{HB}(t)$, $I_H(t)$, $I_B(t)$, $I_{HB}(t)$, and $R_B(t)$ denote the population sizes in each compartment at time t, with total population

$$N(t) = S + V_B + E_H + E_B + E_{HB} + I_H + I_B + I_{HB} + R_B.$$

We define the forces of infection as

$$\lambda_H(t) = \beta_H \frac{I_H(t)}{N(t)}, \qquad \lambda_B(t) = \beta_B \frac{I_B(t)}{N(t)}.$$

Table 1: State variables and definitions.

Variable	Definition
$S(t)$	Susceptible to HIV and HBV
$V_B(t)$	Vaccinated against HBV (fully protected from HBV, still susceptible to HIV)
$E_H(t)$	Exposed/latent HIV (not yet infectious), still at risk of HBV acquisition
$E_B(t)$	Exposed/latent HBV (not yet infectious)
$E_{HB}(t)$	Exposed/latent HBV among HIV-exposed individuals (co-exposed stage)
$I_H(t)$	Infectious with HIV only
$I_B(t)$	Infectious with HBV only
$I_{HB}(t)$	Infectious with HIV–HBV co-infection
$R_B(t)$	Recovered from HBV (permanently immune to HBV)
$N(t)$	Total population size

Table 2: Model parameters, units, and admissible ranges.

Parameter	Definition	Unit	Admissible range
Λ	Recruitment (birth/immigration) rate into S	persons/day	$\Lambda > 0$
μ	Natural mortality rate (all compartments)	1/day	$\mu > 0$
ν	HBV vaccination rate (flow $S \to V_B$)	1/day	$\nu \geq 0$
β_H	Effective HIV transmission rate	1/day	$\beta_H \geq 0$
β_B	Effective HBV transmission rate	1/day	$\beta_B \geq 0$
γ_H	Progression rate $E_H \to I_H$	1/day	$\gamma_H \geq 0$
γ_B	Progression rate $E_B \to I_B$	1/day	$\gamma_B \geq 0$
γ_{HB}	Progression rate $E_{HB} \to I_{HB}$	1/day	$\gamma_{HB} \geq 0$
σ_B	HBV recovery rate $I_B \to R_B$	1/day	$\sigma_B \geq 0$

2.2. Model Equations

The interactions among compartments are described by the following system of differential equations:

$$\begin{aligned}
\frac{dS}{dt} &= \Lambda - \lambda_H S - \lambda_B S - \nu S - \mu S, \\
\frac{dV_B}{dt} &= \nu S - \lambda_H V_B - \mu V_B, \\
\frac{dE_H}{dt} &= \lambda_H (S + V_B) - \lambda_B E_H - \gamma_H E_H - \mu E_H, \\
\frac{dE_B}{dt} &= \lambda_B S - \gamma_B E_B - \mu E_B, \\
\frac{dE_{HB}}{dt} &= \lambda_B E_H - \gamma_{HB} E_{HB} - \mu E_{HB}, \\
\frac{dI_H}{dt} &= \gamma_H E_H - \mu I_H, \\
\frac{dI_B}{dt} &= \gamma_B E_B - \sigma_B I_B - \mu I_B, \\
\frac{dI_{HB}}{dt} &= \gamma_{HB} E_{HB} - \mu I_{HB}, \\
\frac{dR_B}{dt} &= \sigma_B I_B - \mu R_B.
\end{aligned} \tag{1}$$

2.3. Total population dynamics

Summing the system yields

$$\frac{dN}{dt} = \Lambda - \mu N.$$

Therefore, the population is not assumed constant a priori; it approaches the demographic equilibrium $N^* = \Lambda/\mu$ as $t \to \infty$. In analysis and simulations we work at (or near) demographic equilibrium, so $N(t) \approx N^*$ in the incidence terms; in particular, if $N(0) = N^*$ then $N(t) \equiv N^*$ and $\dot{N} = 0$ holds exactly.

2.4. Data usage and model calibration (Kupang, 2008–2023)

The Kupang surveillance data used in this study are reported on an annual basis (yearly totals) for 2008–2023; therefore, model outputs are mapped to annual observables via yearly time-integration of the corresponding incidence flows.

Data sources and observed variables. Annual HIV and HBV surveillance data for Kupang City over 2008–2023 were obtained from local health surveillance reports and routine case notification records [1, 15]. In this study, the observed quantities used for calibration are: (i) annual newly reported HIV cases, denoted by $Y_H(t_k)$; (ii) annual newly reported HBV cases, denoted by $Y_B(t_k)$; and (iii) when available, annual reported HIV–HBV co-infection cases, denoted by $Y_{HB}(t_k)$, for discrete years t_k.

Table 3: Observed data series and their mapping to model outputs.

Observed series	Symbol	Mapped model quantity
Annual new HIV cases	$Y_H(t_k)$	$\widehat{Y}_H(t_k) = \int_{t_k}^{t_{k+1}} \lambda_H(t)\big(S(t) + V_B(t)\big)\, dt$
Annual new HBV cases	$Y_B(t_k)$	$\widehat{Y}_B(t_k) = \int_{t_k}^{t_{k+1}} \lambda_B(t) S(t)\, dt$
Annual new co-infection cases (if available)	$Y_{HB}(t_k)$	$\widehat{Y}_{HB}(t_k) = \int_{t_k}^{t_{k+1}} \lambda_B(t) E_H(t)\, dt$

Mapping rationale. The model is formulated in continuous time, while the surveillance data are reported annually. Therefore, we map each annual observed series to the corresponding model-generated annual incidence proxy obtained by integrating the relevant new-infection flow over each year (Table 3). Specifically, new HIV infections arise from the flow $\lambda_H(S + V_B)$, new HBV infections arise from $\lambda_B S$, and (if co-infection notifications are available) new HBV superinfection among HIV-exposed individuals is represented by the flow $\lambda_B E_H$.

Parameters estimated and fixed quantities. Natural mortality μ and recruitment Λ were set from demographic statistics (with $N^* = \Lambda/\mu$ as the demographic equilibrium). Progression and recovery rates (γ_H, γ_B, γ_{HB}, σ_B) were set from published clinical/epidemiological literature when available [1, 15]. The key transmission parameters β_H and β_B were estimated from the Kupang data. When yearly HBV vaccination coverage data are available, the vaccination rate ν was either fixed accordingly or estimated within admissible bounds.

Calibration method (nonlinear least squares). Let θ denote the parameter vector to be estimated (e.g., $\theta = (\beta_H, \beta_B, \nu)$ or $\theta = (\beta_H, \beta_B)$ when ν is fixed). We estimate θ by minimizing a weighted nonlinear least-squares objective:

$$\begin{aligned} \min_{\theta \in \Theta} J(\theta) \;=\; \sum_k \Big[& w_H \left(\widehat{Y}_H(t_k;\theta) - Y_H(t_k)\right)^2 + w_B \left(\widehat{Y}_B(t_k;\theta) - Y_B(t_k)\right)^2 \\ & + w_{HB} \left(\widehat{Y}_{HB}(t_k;\theta) - Y_{HB}(t_k)\right)^2 \Big] \end{aligned} \tag{2}$$

where $w_H, w_B, w_{HB} \geq 0$ are weights (used to balance the scale of each series), and Θ is the admissible parameter set defined by biologically meaningful bounds (Table 2). The optimization was implemented in MATLAB (using `lsqnonlin` / `fmincon`). Initial conditions at year 2008 were set using the earliest reported counts and demographic totals; unobserved compartment initial values were treated as small fractions and included in a sensitivity check.

Out-of-sample validation and goodness-of-fit. To quantitatively validate the calibrated model, we performed a train–test split: parameters were estimated using data from 2008–2018 (training set), and predictive performance was assessed on 2019–2023 (validation set). We report standard goodness-of-fit metrics for each observed series:

$$\text{RMSE} = \sqrt{\frac{1}{n}\sum_{k=1}^{n}\left(\widehat{Y}(t_k) - Y(t_k)\right)^2}, \tag{3}$$

$$\text{MAPE} = \frac{100}{n}\sum_{k=1}^{n}\left|\frac{\widehat{Y}(t_k) - Y(t_k)}{Y(t_k)}\right|, \tag{4}$$

$$R^2 = 1 - \frac{\sum_k \left(\widehat{Y}(t_k) - Y(t_k)\right)^2}{\sum_k \left(Y(t_k) - \overline{Y}\right)^2}. \tag{5}$$

The resulting fit and validation curves are shown by plotting observed annual cases against the corresponding model-based annual incidence proxies (data vs. model).

3. Results and Discussion

This section presents the analytical and numerical results of the proposed HIV–HBV co-infection model. The discussion begins with the derivation of the basic reproduction number, since this threshold quantity provides the main basis for assessing disease persistence and evaluating subsequent sensitivity, equilibrium, and simulation results.

3.1. Basic reproduction number R_0 (Next Generation Matrix)

To compute the basic reproduction number, we apply the standard Next Generation Matrix (NGM) approach. We consider the infected-state vector consisting of the compartments involved in the production of new infections near the disease-free equilibrium (DFE):

$$x(t) = \left(E_H(t),\, I_H(t),\, E_B(t),\, I_B(t)\right)^T. \tag{6}$$

Note that the co-infection exposure class E_{HB} is generated through the bilinear term $\lambda_B E_H$, which is of higher order around the DFE (since $E_H = 0$ at the DFE). Therefore E_{HB} and I_{HB} do not contribute to the linearized infected subsystem used in the NGM construction.

1. Disease-free equilibrium (DFE)

Setting all infected compartments to zero gives the DFE:

$$D_0 = (S^*, V_B^*, 0, 0, 0, 0, 0, 0, 0), \tag{7}$$

with

$$S^* = \frac{\Lambda}{\nu + \mu}, \tag{8}$$

$$V_B^* = \frac{\nu}{\mu}S^* = \frac{\nu\Lambda}{\mu(\nu + \mu)}, \tag{9}$$

$$N^* = \frac{\Lambda}{\mu}. \tag{10}$$

Hence,

$$\frac{S^*}{N^*} = \frac{\mu}{\nu+\mu}, \tag{11}$$

$$\frac{S^*+V_B^*}{N^*} = 1. \tag{12}$$

2. Construction of F and V

Write the infected subsystem in the form $\dot{x} = \mathcal{F}(x) - \mathcal{V}(x)$, where $\mathcal{F}$ collects the rates of appearance of new infections and $\mathcal{V}$ collects all other transitions. Using $\lambda_H = \beta_H I_H/N$ and $\lambda_B = \beta_B I_B/N$, the new infection terms are:

$$\mathcal{F}_1 = \lambda_H(S+V_B), \qquad \mathcal{F}_2 = 0, \qquad \mathcal{F}_3 = \lambda_B S, \qquad \mathcal{F}_4 = 0. \tag{13}$$

The remaining transition terms are:

$$\mathcal{V}_1 = (\gamma_H+\mu)E_H, \tag{14}$$

$$\mathcal{V}_2 = \mu I_H - \gamma_H E_H, \tag{15}$$

$$\mathcal{V}_3 = (\gamma_B+\mu)E_B, \tag{16}$$

$$\mathcal{V}_4 = (\sigma_B+\mu)I_B - \gamma_B E_B. \tag{17}$$

Let F and V denote the Jacobian matrices of $\mathcal{F}(x)$ and $\mathcal{V}(x)$ evaluated at the DFE. With the ordering $x = (E_H, I_H, E_B, I_B)^T$, we obtain:

$$F = \begin{pmatrix} 0 & \beta_H\frac{S^*+V_B^*}{N^*} & 0 & 0 \\ 0 & 0 & 0 & 0 \\ 0 & 0 & 0 & \beta_B\frac{S^*}{N^*} \\ 0 & 0 & 0 & 0 \end{pmatrix} = \begin{pmatrix} 0 & \beta_H & 0 & 0 \\ 0 & 0 & 0 & 0 \\ 0 & 0 & 0 & \beta_B\frac{\mu}{\nu+\mu} \\ 0 & 0 & 0 & 0 \end{pmatrix}, \tag{18}$$

and

$$V = \begin{pmatrix} \gamma_H+\mu & 0 & 0 & 0 \\ -\gamma_H & \mu & 0 & 0 \\ 0 & 0 & \gamma_B+\mu & 0 \\ 0 & 0 & -\gamma_B & \sigma_B+\mu \end{pmatrix}. \tag{19}$$

3. Definition of R_0 and Decomposition

The next-generation matrix is $K = FV^{-1}$ and the basic reproduction number is defined by

$$R_0 = \rho(K) = \rho(FV^{-1}), \tag{20}$$

where $\rho(\cdot)$ is the spectral radius. Since F and V are block diagonal with respect to the HIV and HBV subsystems, K is also block diagonal and the decomposition is rigorous. The subsystem reproduction numbers are:

$$R_H = \frac{\beta_H\,\gamma_H}{\mu(\gamma_H+\mu)}, \tag{21}$$

$$R_B = \left(\beta_B\frac{S^*}{N^*}\right)\left(\frac{\gamma_B}{\gamma_B+\mu}\right)\left(\frac{1}{\sigma_B+\mu}\right) = \beta_B\left(\frac{\mu}{\nu+\mu}\right)\left(\frac{\gamma_B}{\gamma_B+\mu}\right)\left(\frac{1}{\sigma_B+\mu}\right), \tag{22}$$

and therefore

$$R_0 = \max\{R_H,\, R_B\}. \tag{23}$$

4. Baseline Numerical Evaluation

Using the baseline parameter values in Table 4 (the same set used in the simulations), we compute R_H and R_B by direct substitution and obtain:

$$R_0 = \max\{R_H,\, R_B\} = 1.36. \tag{24}$$

Table 4: Baseline parameter values used to compute R_0 (and used in simulations).

Parameter	Description	Unit	Baseline value
β_H	HIV transmission rate	1/day	3.0×10^{-5}
β_B	HBV transmission rate	1/day	2.07×10^{-2}
γ_H	Progression rate $E_H \to I_H$	1/day	1.0×10^{-1}
γ_B	Progression rate $E_B \to I_B$	1/day	2.0×10^{-2}
σ_B	HBV recovery rate $I_B \to R_B$	1/day	1.0×10^{-2}
ν	HBV vaccination rate $S \to V_B$	1/day	2.0×10^{-5}
μ	Natural mortality rate	1/day	3.9×10^{-5}

3.2. Sensitivity analysis

To identify the parameters that most influence transmission potential, we perform a *normalized forward sensitivity analysis* of the basic reproduction number R_0. For a parameter p, the normalized forward sensitivity index of R_0 with respect to p is defined as

$$\Upsilon_p^{R_0} = \frac{p}{R_0}\frac{\partial R_0}{\partial p}. \tag{25}$$

A positive value of $\Upsilon_p^{R_0}$ indicates that increasing p increases R_0, while a negative value indicates that increasing p decreases R_0. The magnitude $|\Upsilon_p^{R_0}|$ measures the relative importance of p: for example, $\Upsilon_p^{R_0} = 1$ means that a 1% increase in p produces approximately a 1% increase in R_0.

Since $R_0 = \max\{R_H, R_B\}$ (Section on R_0), sensitivity indices are computed with respect to the dominant component. In our baseline setting, the HBV component R_B dominates (yielding $R_0 = R_B$), so the indices below are computed for R_B. Using

$$R_B = \beta_B \left(\frac{\mu}{\nu+\mu}\right)\left(\frac{\gamma_B}{\gamma_B+\mu}\right)\left(\frac{1}{\sigma_B+\mu}\right), \tag{26}$$

we obtain the following sensitivity indices:

$$\begin{aligned}
\Upsilon_{\beta_B}^{R_0} &= 1, \\
\Upsilon_{\nu}^{R_0} &= -\frac{\nu}{\nu+\mu}, \\
\Upsilon_{\gamma_B}^{R_0} &= \frac{\mu}{\gamma_B+\mu}, \\
\Upsilon_{\sigma_B}^{R_0} &= -\frac{\sigma_B}{\sigma_B+\mu}, \\
\Upsilon_{\mu}^{R_0} &= 1 - \frac{\mu}{\nu+\mu} - \frac{\mu}{\gamma_B+\mu} - \frac{\mu}{\sigma_B+\mu}.
\end{aligned} \tag{27}$$

For completeness, if the HIV component dominates ($R_0 = R_H$), then with

$$R_H = \frac{\beta_H \gamma_H}{\mu(\gamma_H+\mu)}, \tag{28}$$

the corresponding indices are

$$\Upsilon_{\beta_H}^{R_0} = 1, \tag{29}$$

$$\Upsilon_{\gamma_H}^{R_0} = \frac{\mu}{\gamma_H+\mu}, \tag{30}$$

$$\Upsilon_{\mu}^{R_0} = -1 - \frac{\mu}{\gamma_H+\mu}. \tag{31}$$

Standardized sensitivity table. Table 5 reports the baseline parameter values used in simulations together with the normalized forward sensitivity indices computed at the baseline.

Table 5: Normalized forward sensitivity indices of R_0 evaluated at baseline parameters.

Parameter	Description	Baseline value	$\Upsilon_p^{R_0}$
β_B	HBV transmission rate	3.9×10^{-5}	1
ν	HBV vaccination rate	1.0×10^{-4}	$-\frac{\nu}{\nu+\mu}$
γ_B	Progression $E_B \to I_B$	$1.67 \times 10^{-2} (\approx 1/60)$	$\frac{\mu}{\gamma_B+\mu}$
σ_B	HBV recovery $I_B \to R_B$	$1.11 \times 10^{-2} (\approx 1/90)$	$-\frac{\sigma_B}{\sigma_B+\mu}$
μ	Natural mortality rate	5.4×10^{-2}	$1 - \frac{\mu}{\nu+\mu} - \frac{\mu}{\gamma_B+\mu} - \frac{\mu}{\sigma_B+\mu}$

Why only a subset of parameters is reported. Although R_0 depends on multiple parameters, we report sensitivity indices for the dominant and policy-actionable parameters with the largest absolute influence under the baseline regime. These include the HBV transmission rate β_B, the HBV vaccination rate ν, the HBV progression rate γ_B, and the HBV recovery/treatment rate σ_B. Other parameters were fixed from demographic statistics or clinical literature and exhibited smaller influence on R_0 at baseline.

Computation method and interpretation of negative indices. Sensitivity indices are computed using the normalized forward sensitivity definition in Eq. (25) by differentiating the closed-form expression of the dominant component of R_0 (either R_H or R_B) with respect to each parameter and then evaluating the result at the baseline parameter set. Importantly, negative values in the sensitivity table refer to the sensitivity indices $\Upsilon_p^{R_0}$, not to the parameter values. All model parameters are nonnegative by definition (Table 2). A negative sensitivity index simply indicates an inverse relationship: increasing the parameter decreases R_0. For example, $\Upsilon_\nu^{R_0} < 0$ means increasing HBV vaccination reduces transmission potential, and $\Upsilon_{\sigma_B}^{R_0} < 0$ means improving HBV recovery/treatment reduces R_0.

Interpretation. We focus on a small subset of parameters in the sensitivity table for two reasons. First, these parameters have the largest absolute normalized sensitivity indices at the baseline and therefore dominate the variability of R_0. Second, they correspond to actionable public-health levers (vaccination uptake ν, transmission reduction via β_H or β_B, and HBV treatment/recovery σ_B). Other parameters were fixed from demographic statistics or clinical literature and showed smaller influence under the baseline regime.

The most influential parameters are those with the largest $|\Upsilon_p^{R_0}|$. In particular, β_B has $\Upsilon_{\beta_B}^{R_0} = 1$, meaning a 1% reduction in HBV transmission produces approximately a 1% reduction in R_0. The vaccination rate ν has a negative sensitivity index, confirming that increasing vaccination coverage reduces R_0. Very large (in magnitude) indices can occur when R_0 depends strongly on a parameter and/or when the baseline of that parameter is small, so that a small absolute change corresponds to a large relative change. This underscores that improving HBV vaccination uptake and reducing HBV transmission (e.g., through prevention programs) are high-impact interventions. Similarly, increasing the HBV recovery/treatment rate σ_B decreases R_0, supporting the importance of improving access to HBV diagnosis and treatment.

3.3. Equilibrium Analysis

This section summarizes equilibrium points of the HIV–HBV co-infection model (Eq. (1)) using consistent notation and provides a concise stability argument based on the NGM threshold. Let

$$X(t) = \big(S(t),\, V_B(t),\, E_H(t),\, E_B(t),\, E_{HB}(t),\, I_H(t),\, I_B(t),\, I_{HB}(t),\, R_B(t)\big)^T \in \mathbb{R}_+^9, \tag{32}$$

with total population

$$N(t) = S + V_B + E_H + E_B + E_{HB} + I_H + I_B + I_{HB} + R_B. \tag{33}$$

Summing the equations in Eq. (1) yields $\dot{N} = \Lambda - \mu N$, hence at any equilibrium $N^* = \Lambda/\mu$.

1. Disease-Free Equilibrium (DFE)

To avoid confusion with time-dependent variables, we denote the DFE components with subscript "0". At the DFE, all infection-related compartments vanish:

$$E_{H0} = E_{B0} = E_{HB0} = I_{H0} = I_{B0} = I_{HB0} = R_{B0} = 0. \tag{34}$$

Setting $\dot{S} = \dot{V}_B = 0$ in Eq. (1) gives

$$0 = \Lambda - (\nu + \mu)S_0, \tag{35}$$
$$0 = \nu S_0 - \mu V_{B0}, \tag{36}$$

so that

$$S_0 = \frac{\Lambda}{\nu + \mu}, \tag{37}$$
$$V_{B0} = \frac{\nu}{\mu} S_0 = \frac{\nu\Lambda}{\mu(\nu + \mu)}. \tag{38}$$

Therefore, the DFE is the 9-dimensional vector

$$D_0 = (S_0, V_{B0}, 0, 0, 0, 0, 0, 0, 0). \tag{39}$$

2. Stability of the DFE and threshold quantities

Let $R_0 = \rho(FV^{-1})$ be the basic reproduction number obtained from the NGM construction (see the R_0 subsection). By the standard NGM theorem [17], the DFE D_0 is locally asymptotically stable if $R_0 < 1$ and unstable if $R_0 > 1$. In this model, the invasion thresholds can be written as the contributions of HIV and HBV pathways:

$$R_0 = \max\{R_H, R_B\}. \tag{40}$$

A convenient biological interpretation is that the overall invasion potential is governed by the dominant transmission mechanism: if either $R_H > 1$ or $R_B > 1$, then D_0 loses stability and the corresponding infection can persist.

3. Role of Parameters in R_H and R_B

At the DFE, $N_0 = \Lambda/\mu$ and $S_0/N_0 = \mu/(\nu+\mu)$, so increasing vaccination ν reduces the susceptible fraction. A standard generation-counting argument yields the explicit dependence

$$R_H = \frac{\beta_H}{\mu} \frac{S_0 + V_{B0}}{N_0} \frac{\gamma_H}{\gamma_H + \mu}, \tag{41}$$
$$R_B = \frac{\beta_B}{\sigma_B + \mu} \frac{S_0}{N_0} \frac{\gamma_B}{\gamma_B + \mu}. \tag{42}$$

Thus, β_H and β_B increase invasion potential, while vaccination ν decreases R_B through S_0/N_0, and improved HBV recovery/treatment σ_B decreases R_B through the factor $(\sigma_B + \mu)^{-1}$.

4. Endemic equilibrium (EE)

We denote endemic equilibrium components with superscript "+":

$$E^+ = (S^+, V_B^+, E_H^+, E_B^+, E_{HB}^+, I_H^+, I_B^+, I_{HB}^+, R_B^+), \tag{43}$$

where at least one infectious class is positive (e.g., $I_H^+ > 0$ and/or $I_B^+ > 0$).

To avoid duplicated algebra, the EE is specified implicitly by the steady-state system $\dot{X} = 0$ applied to Eq. (**??**). In particular, the exposed–infectious relations can be written compactly as

$$E_H^+ = \frac{\lambda_H^+(S^+ + V_B^+ + R_B^+)}{\gamma_H + \mu}, \qquad I_H^+ = \frac{\gamma_H}{\mu} E_H^+, \tag{44}$$

$$E_B^+ = \frac{\lambda_B^+ S^+}{\gamma_B + \mu}, \qquad I_B^+ = \frac{\gamma_B}{\sigma_B + \mu} E_B^+, \tag{45}$$

$$E_{HB}^+ = \frac{\lambda_B^+ I_H^+}{\gamma_{HB} + \mu}, \qquad I_{HB}^+ = \frac{\gamma_{HB}}{\mu} E_{HB}^+, \tag{46}$$

where the forces of infection at equilibrium are

$$\lambda_H^+ = \frac{\beta_H(I_H^+ + \kappa_H I_{HB}^+)}{N^+}, \qquad \lambda_B^+ = \frac{\beta_B(I_B^+ + \kappa_B I_{HB}^+)}{N^+}, \qquad N^+ = \frac{\Lambda}{\mu}. \tag{47}$$

5. Existence and stability interpretation

The DFE always exists. If $R_0 < 1$, then D_0 is stable and infections die out. If $R_0 > 1$, then D_0 is unstable and the system may approach an endemic regime. In particular, $R_H > 1$ supports persistence of HIV transmission, $R_B > 1$ supports persistence of HBV transmission, and when both exceed one the dynamics may exhibit co-endemic persistence, which is explored numerically in the simulation section.

3.4. Numerical Simulation

Numerical simulations were conducted using MATLAB R2023a software to validate the theoretical model and explore various intervention scenarios. Different hypothetical scenarios were systematically analyzed, including a baseline scenario with no interventions, increased HBV vaccination coverage, enhanced HBV treatment accessibility, and a combined strategy incorporating both increased vaccination and improved treatment. The results are displayed in Fig. 2.

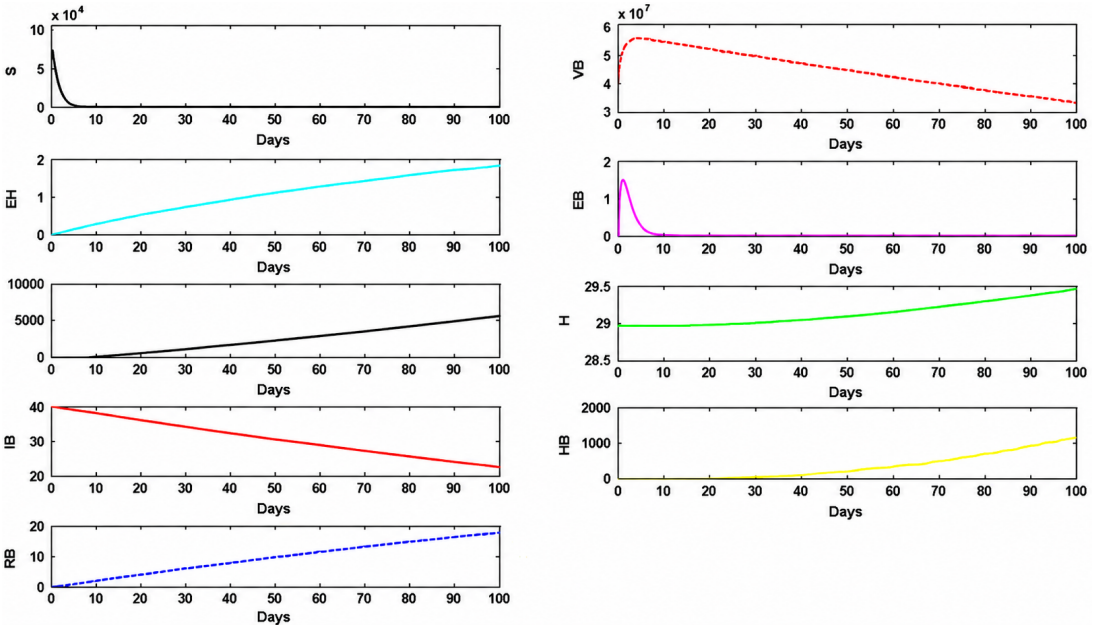

Fig. 2: Numerical Simulation of SVEIR Model for Human Population in Kupang City

The baseline scenario predicted a continual rise in co-infection prevalence, clearly indicating the urgent necessity for intervention implementation. Doubling the vaccination rate substantially decreased HBV prevalence, consequently lowering co-infection rates significantly. Similarly,

enhancing HBV treatment accessibility by increasing recovery rates by 50% demonstrated notable reductions in the prevalence of infection. The combined intervention scenario provided the most pronounced reduction in infection rates, confirming that a multifaceted approach—combining vaccination and treatment accessibility—offers the most effective public health strategy to reduce HIV-HBV co-infection prevalence, aligning closely with recent epidemiological findings and recommendations [3, 8].

3.5. Summary of Key Finding

Based on the outcomes of this study, several significant implications emerge for public health policy and interventions in Kupang City. Primarily, the study emphasizes the necessity of expanding hepatitis B vaccination programs, as increased vaccination coverage has been clearly demonstrated to significantly reduce the risk of HIV-HBV co-infection. Enhanced access to hepatitis B antiviral treatment is equally crucial, as adequate treatment availability can substantially elevate recovery rates, consequently reducing disease transmission. Additionally, community education and awareness campaigns are essential to inform the public about the risks associated with unsafe sexual behaviors, intravenous drug use, and the critical importance of early detection and regular health screenings. Furthermore, integrated HIV-HBV control programs that combine preventive strategies, such as vaccination and education, with ongoing monitoring and treatment can optimize public health resources and improve health outcomes. Several key findings support these recommendations. The basic reproduction number (R_0), estimated at 1.36, underscores the ongoing potential for disease spread if left unaddressed. Specifically, hepatitis B transmission and progression rates were identified as particularly influential in driving infection dynamics, suggesting that targeted interventions aimed at reducing transmission routes and enhancing early treatment could significantly curtail disease prevalence. The study's numerical simulations further confirm that interventions focusing on increased vaccination rates and improved access to hepatitis B treatments yield the most effective results. Thus, it is recommended that public health initiatives prioritize these strategies. Ultimately, these integrated approaches not only enhance disease control but also contribute positively to the overall health status of the community.

3.6. Interpretation of Key Findings and Public Health Implication

The results of this study provide significant insights into the dynamics and control strategies associated with HIV-HBV co-infection in Kupang City. A key finding from the analysis is the estimated basic reproduction number (R_0) of 1.36, indicating that, on average, each infected individual can transmit the infection to more than one person. This R_0 value underscores the necessity of effective and targeted public health interventions; without intervention, the disease transmission is expected to remain persistent and endemic within the community. A similar observation was reported by [18], who demonstrated that even with a basic reproduction number below one, disease elimination is not guaranteed due to the phenomenon of backward bifurcation, especially in contexts with unequal access to healthcare services.

These findings align closely with existing literature on co-infection dynamics, particularly the documented acceleration of disease progression in HIV-HBV co-infected individuals compared to those infected with HBV alone [19, 20]. Previous studies, such as those by [11] and [12], similarly emphasized the utility of mathematical modeling in understanding co-infection dynamics, although these studies primarily addressed HIV-HCV co-infections without conducting comprehensive sensitivity analyses. In contrast, this study includes a robust sensitivity analysis, similar to the approach taken by [21], who used spectral collocation methods to solve HIV infection models and emphasized the importance of numerical accuracy in capturing disease dynamics. This study, however, incorporates sensitivity analyses, providing a deeper understanding of the relative impacts of different transmission and intervention parameters. This methodological advancement offers a nuanced perspective, significantly enhancing predictions and informing targeted control strategies [10].

Additionally, the results from numerical simulations reinforce the crucial role of vaccination and antiviral therapy accessibility in controlling disease transmission. Simulations demonstrated that increasing HBV vaccination coverage substantially reduces HBV prevalence and, consequently, co-infection rates, confirming observations in recent global analyses [8]. Improved accessibility to antiviral treatments further demonstrated a significant reduction in the overall infection rates, aligning with clinical studies advocating integrated care approaches for managing HIV-HBV co-infections [5].

The policy implications derived from this study are directly relevant to Kupang City and similar high-risk areas. Foremost among these recommendations is the expansion of HBV vaccination programs, particularly targeting newborns and high-risk adults, which has shown significant potential in reducing HBV transmission. Enhancing access to antiviral treatments for both HIV and HBV is equally crucial, given the documented effectiveness of comprehensive treatment programs in reducing co-infection morbidity and mortality rates. Furthermore, community awareness campaigns highlighting safe sexual practices, dangers associated with needle sharing, and importance of early vaccination and screening are critical components of effective public health interventions. These integrated control measures, supported by existing literature and corroborated by this study's findings, present robust strategies for controlling HIV-HBV co-infection and improving population health outcomes.

3.7. Limitations and Future Research Directions

While this study provides valuable insights into the transmission dynamics and control strategies of HIV-HBV co-infection in Kupang City, certain limitations should be acknowledged. The modeling approach employed in this research relies on several simplifying assumptions, such as constant population size and homogeneous mixing of individuals, which may not accurately represent the complex and heterogeneous nature of real-world populations. Additionally, the study's dependence on historical epidemiological data collected from Kupang City between 2008 and 2023 might not fully capture variations across different regions or reflect more recent epidemiological shifts, particularly in rural or underserved areas. Behavioral factors, such as socioeconomic status, healthcare accessibility, public awareness, and stigma—elements known to significantly influence infection dynamics—were not explicitly included in the model. Moreover, underreporting due to limited diagnostic facilities and healthcare access likely results in an underestimated actual infection burden within the community.

To enhance the robustness and applicability of future modeling studies on HIV-HBV co-infection, researchers are encouraged to incorporate individual-based modeling approaches, which can more effectively capture population heterogeneity and specific individual behaviors. Future investigations should also consider exploring the impact of antiviral resistance, as resistance patterns could substantially affect treatment effectiveness and disease control efforts. Moreover, integrating socioeconomic and behavioral determinants of health into mathematical models could greatly enhance the predictive accuracy and practical applicability of results. Expanded data collection efforts through comprehensive longitudinal studies across diverse regions are necessary to improve our understanding of disease trends and refine predictive models. Addressing these considerations in future research will significantly advance our capability to design targeted and effective intervention strategies, thereby improving public health outcomes in Kupang City and similar contexts.

4. Conclusion

This study utilized the SVEIR model to comprehensively investigate HIV-HBV co-infection dynamics in Kupang City, Indonesia. The estimated basic reproduction number ($R_0 = 1.36$) confirmed ongoing disease transmission and highlighted the urgent need for targeted interventions. Sensitivity analyses underscored the importance of HBV vaccination and improved antiviral treatment accessibility in reducing co-infection prevalence. Numerical simulations further sup-

ported the effectiveness of combined vaccination and treatment strategies, reinforcing their role in achieving disease control. The findings strongly advocate for integrated public health measures, including expanded vaccination programs, enhanced antiviral treatment access, and community awareness initiatives. While the current model provided robust insights, future studies should incorporate behavioral, socioeconomic, and antiviral resistance factors to refine predictions and intervention strategies. Ultimately, these integrated approaches will significantly improve public health outcomes and contribute to controlling HIV-HBV co-infection within affected communities.

CRediT Authorship Contribution Statement

Maria Lobo: Conceptualization, Methodology, Formal analysis, Investigation, Software, Writing–original draft, Visualization, Supervision, Project administration. **Adelya Hanaya Mage:** Data curation, Formal analysis, Validation, Writing–review & editing, Visualization. **Ariyanto:** Methodology, Software, Validation, Writing–review & editing, Supervision.

Declaration of Generative AI and AI-assisted technologies

During the preparation of this manuscript, the authors used ChatGPT (OpenAI) for language editing and improving readability (e.g., grammar, clarity, and academic style). All scientific content, data interpretation, and conclusions were developed and verified by the authors. The authors take full responsibility for the integrity and accuracy of the work.

Declaration of Competing Interest

The authors declare that they have no competing interests.

Funding and Acknowledgments

This research received no external funding. The authors acknowledge the support of the Faculty of Science and Engineering, Department of Mathematics, Nusa Cendana University. The authors also acknowledge the use of MATLAB R2023a for numerical simulations.

Data and Code Availability

The data supporting the findings of this study are derived from the sources described in the manuscript and from computations performed in this work. The MATLAB scripts used to generate the numerical simulations and reproduce the results are available from the corresponding author upon reasonable request (E-mail: maria_lobo@staf.undana.ac.id).

References

[1] Joint United Nations Programme on HIV/AIDS (UNAIDS). *Global HIV & AIDS statistics – Fact sheet 2021*. Report. 2021.

[2] World Health Organization. *Global hepatitis report 2017*. Geneva: WHO, 2017. https://www.afro.who.int/sites/default/files/2017-06/9789241565455-eng.pdf.

[3] L. Platt et al. "Prevalence and burden of HBV co-infection among people living with HIV: A global systematic review and meta-analysis". In: *Journal of Viral Hepatitis* 27.3 (2019). https://doi.org/10.1111/jvh.13217, pp. 294–315.

[4] Y. Wondimeneh, M. Alem, F. Asfaw, and Y. Belyhun. "HBV and HCV seroprevalence and their correlation with CD4 cells and liver enzymes among HIV positive individuals at University of Gondar Teaching Hospital, Northwest Ethiopia". In: *Virology Journal* 10.1 (2013). https://doi.org/10.1186/1743-422x-10-171.

[5] H. Hethcote. "The Mathematics of Infectious Diseases". In: *Siam Review* 42.4 (2000). https://doi.org/10.1137/s0036144500371907, pp. 599–653.

[6] G. Chowell, L. Sattenspiel, S. Bansal, and C. Viboud. "Mathematical models to characterize early epidemic growth: A review". In: *Physics of Life Reviews* 18 (2016). https://doi.org/10.1016/j.plrev.2016.07.005, pp. 66–97.

[7] C. Weinbaum, E. Mast, and J. Ward. "Recommendations for identification and public health management of persons with chronic hepatitis B virus infection". In: *Hepatology* 49.5 (2009). https://doi.org/10.1002/hep.22882, S35–S44.

[8] Z. Cheng, P. Lin, and N. Cheng. "HBV/HIV Coinfection: Impact on the Development and Clinical Treatment of Liver Diseases". In: *Frontiers in Medicine* 8 (2021). https://doi.org/10.3389/fmed.2021.713981.

[9] S. Marino, I. Hogue, J. Ray, and D. Kirschner. "A methodology for performing global uncertainty and sensitivity analysis in systems biology". In: *Journal of Theoretical Biology* 254.1 (2008). https://doi.org/10.1016/j.jtbi.2008.04.011, pp. 178–196.

[10] T. Zhang, K. Wang, and X. Zhang. "Modeling and Analyzing the Transmission Dynamics of HBV Epidemic in Xinjiang, China". In: *Plos One* 10.9 (2015). https://doi.org/10.1371/journal.pone.0138765, e0138765.

[11] E. Mayanja, L. Luboobi, J. Kasozi, and R. Nsubuga. "Mathematical Modelling of HIV-HCV Coinfection Dynamics in Absence of Therapy". In: *Computational and Mathematical Methods in Medicine* 2020 (2020). https://doi.org/10.1155/2020/2106570, pp. 1–27.

[12] O. Abiodun, O. Adebimpe, J. Ndako, O. Oludoun, B. Aladeitan, and M. Adeniyi. "Mathematical modeling of HIV-HCV co-infection model: Impact of parameters on reproduction number". In: *F1000research* 11 (2022). https://doi.org/10.12688/f1000research.124555.2, p. 1153.

[13] H. Jin, S. Chen, and Z. Li. "Dynamic Analysis and Optimal Control of a Stochastic SVEIRS Model With Saturation Incidence". In: *Mathematical Methods in the Applied Sciences* 48.11 (2025). https://doi.org/10.1002/mma.10975, pp. 11455–11472.

[14] X. Wang, L. Zhang, and X. Zhang. "Dynamics of a Stochastic SVEIR Epidemic Model with Nonlinear Incidence Rate". In: *Symmetry* 16.4 (2024). https://doi.org/10.3390/sym16040467, p. 467.

[15] World Health Organization (WHO). *Global Hepatitis Report 2023*. Available at: https://www.who.int. Geneva, Switzerland, 2023.

[16] M. Chang and D. Chen. "Prevention of Hepatitis B". In: *Cold Spring Harbor Perspectives in Medicine* 5.3 (2015). https://doi.org/10.1101/cshperspect.a021493, a021493–a021493.

[17] P. van den Driessche and James Watmough. "Reproduction numbers and sub-threshold endemic equilibria for compartmental models of disease transmission". In: *Mathematical Biosciences* 180.1 (2002). https://doi.org/10.1016/S0025-5564(02)00108-6, pp. 29–48.

[18] Salihu Sabiu Musa, Shi Zhao, Nafiu Hussaini, Abdulrazaq G. Habib, and Daihai He. "Mathematical Modeling and Analysis of Meningococcal Meningitis Transmission Dynamics". In: *International Journal of Biomathematics* 13.2 (2020), p. 2050006. DOI: 10.1142/S1793524520500060.

[19] K. Singh, M. Crane, J. Audsley, A. Avihingsanon, J. Sasadeusz, and S. Lewin. "HIV-hepatitis B virus coinfection". In: *Aids* 31 (15 2017). https://doi.org/10.1097/qad.0000000000001574, pp. 2035–2052.

[20] C. Thio et al. "Characterization of HIV–HBV coinfection in a multinational HIV-infected cohort". In: *Aids* 27 (2 2013). https://doi.org/10.1097/qad.0b013e32835a9984, pp. 191–201.

[21] Sagithya Thirumalai, Rajeswari Seshadri, and Suayip Yuzbasi. "On the Solution of the Human Immunodeficiency Virus (HIV) Infection Model Using Spectral Collocation Method". In: *International Journal of Biomathematics* 13.2 (2020). https://doi.org/10.1142/S1793524520500746, p. 2050074.